Quantum tunneling in nonintegrable systems: beyond the leading order semiclassical description (Several aspects of microlocal analysis)

AUTHOR(S):

Shudo, Akira; Hanada, Yasutaka; Ikeda, Kensuke S.

RIMS Kôkyûroku Bessatsu
B57 (2016), 027–038

Quantum tunneling in nonintegrable systems: beyond the leading order semiclassical description

By

Akira SHUDO*, Yasutaka HANADA** and Kensuke S. IKEDA***

Abstract

Quantum tunneling in the system with mixed phase space is studied based on the saddle point approximation of quantum one-step propagator. If the phase space is sharply or almost sharply divided into regular and chaotic components, it is found that diffraction dominates in the transition process rather than tunneling. The latter is the phenomenon described by the saddle points of propagator, whereas the former is regarded as the one beyond the leading-order description of saddle point analysis.

§ 1. Introduction

Generic Hamiltonian systems are neither completely integrable nor ideally chaotic, and the phase space is a mixture of regular and chaotic components, which are generally intermingled with each other in a single phase space. The mixed phase space provokes a wealth of interesting questions in the corresponding quantum mechanics. Among them, we here pay our attention to *dynamical tunneling* [1, 2]. Dynamical tunneling is referred to as classically forbidden thus purely quantum phenomena which emerge in mixed phase space. To see a direct and close connection between signatures of dynamical tunneling and the underlying classical dynamics, one may expect that the semiclassical or WKB approach could play the same role as in the analysis which has worked as a bridge between classical and quantum mechanics in chaotic systems. Note that "semiclassical"

Received May 7, 2015. Revised September 30, 2015. Accepted September 30, 2015.
2010 Mathematics Subject Classification(s): 34E20, 37D20
Key Words: *Quantum tunneling, Chaos, Saddle point method, Diffraction.*
*Department of Physics, Tokyo Metropolitan University, Minami-Osawa, Hachioji, Tokyo 192-0397, Japan. e-mail: shudo@tmu.ac.jp
**Department of Physics, Tokyo Metropolitan University, Minami-Osawa, Hachioji, Tokyo 192-0397, Japan. e-mail: hanada.yasutaka@gmail.com
***Department of Physics, Ritsumeikan University, Kusatsu, Shiga 525-0577, Japan. e-mail: ahoo@amber.plala.or.jp

or "WKB" is here being used as the term for generic asymptotic expansions involving exponentials, not only for differential equations, but for the saddle point evaluation of integrals.

For mixed systems, it is well known that no semiclassical formula exists in the energy domain such as the Gutzwiller trace formula for hyperbolic systems, or the Berry-Tabor formula for completely integrable systems. Therefore, we can at best take time-domain semiclassical analysis, based on Van Vleck-Gutzwiller-type propagator. We have indeed spent many years in performing the time-domain semiclassical analysis based on complex classical dynamics, and found that complex semiclassical analyses work well within the leading order [3, 4, 5, 6, 7].

However, as actually discussed below, the leading order time-domain semiclassical calculation does not always work. This fact has not so explicitly been recognized so far, but our recent work is revealing that the time-domain propagator, not necessarily in multiple steps but only in a single step, exhibits quite an anomalous behavior. What is more, such an anomaly is closely linked to drastic enhancement of tunneling in non-integrable systems [8]. Therefore, exploring the origin of anomaly in the time-domain propagator now becomes quite a significant issue for our understanding of quantum tunneling in mixed phase space.

Here we shall perform not long time, but just a single step semiclassical analysis, by setting the initial and final states to be as close as possible to the energy domain by adjusting the representations in a proper way. In particular, as explained below the *action* representation plays a crucial role and the leading-order semiclassical approximation could break when the supports of initial and final states are close enough to the underlying invariant manifolds.

§ 2. Map with continuity

We consider the following area-preserving map [9]:

$$F : \begin{pmatrix} p' \\ q' \end{pmatrix} = \begin{pmatrix} p - V'(q) \\ q + T'(p') \end{pmatrix} \tag{2.1}$$

where

$$T(p) = T_0(p) + T_1(p) \tag{2.2}$$

$$V(q) = K\cos(2\pi q) \tag{2.3}$$

and $T_0(p)$ and $T_1(p)$ are respectively given as

$$T_0(p) = \omega(p - d) \tag{2.4}$$

$$T_1(p) = \left[\frac{s}{2}(p-d)^2 + g(p-d)\right]\theta_\beta(p-d). \tag{2.5}$$

Here we introduce the smoothed step function $\theta_\beta(p)$ as

$$\theta_\beta(p) \equiv \frac{1}{2}\Big[\tanh(\beta p) + 1\Big]\,. \tag{2.6}$$

The parameter β controls the sharpness of the kinetic term $T_1(p)$. As shown in Fig. 1 the phase space is split into regular and chaotic regions, and the border becomes sharper as the value of β increases. Note however that the border looks strictly sharp in the case of $\beta = \infty$, like the so-called mushroom billiards, but this is not the case.

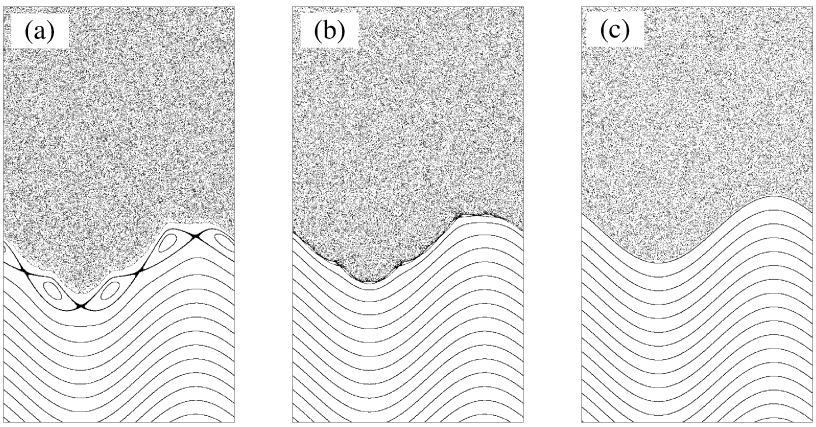

Figure 1. Classical phase space for the map (2.1) with (a) $\beta = 0.1$, (b) $\beta = 2$ and (c) $\beta = \infty$.

One-step time propagation from an initial to a final state, or alternatively, the matrix element in certain representations is a fundamental building block in constructing quantum mechanics of the area-preserving map. Here we especially focus on one-step propagator in the *action* representation:

$$\langle I'|\hat{\mathcal{U}}\,|I\rangle = \int_{-\infty}^{\infty} dq \int_{-\infty}^{\infty} dq' \int_{-\infty}^{\infty} dp \exp\left[-\frac{\mathrm{i}}{\hbar}\Big\{F(q',p,q;I,I')\Big\}\right] \tag{2.7}$$

where

$$F(q',p,q;I,I') := S(I',q') - S(I,q) - p(q'-q) + T(p) + V(q)\,. \tag{2.8}$$

Here $S(I,q)$ represents the generating function for the canonical transformation from (q,p) to (θ,I). In the present case we have

$$S(I,q) = \int^{q} p'(I,q)dq' = Iq + a\sin\big(q - \frac{\omega}{2}\big) \tag{2.9}$$

where $a = K/\sin(\omega/2)$. Note that the state $|\,I\,\rangle$ denotes the eigenfunction for the linear map: $\hat{\mathcal{U}}_0|\,I_n\rangle = \mathrm{e}^{-\frac{\mathrm{i}}{\hbar}E_n}|\,I_n\rangle$ where $\hat{\mathcal{U}}_0 = \mathrm{e}^{-\frac{\mathrm{i}}{\hbar}\omega p}\mathrm{e}^{-\frac{\mathrm{i}}{\hbar}K\sin q}$.

As shown in Fig. 2, the nature of one-step propagator in the action representation strongly depends on the smoothness parameter β. For a small β case, $|\langle I'|\hat{\mathcal{U}}\,|I\rangle|^2$ decays

exponentially, whereas there appears the plateau, whose center is located around the border between regular and chaotic regions for large β cases. The former is a typical signature of quantum tunneling and indeed can be reproduced by applying the standard saddle point approximation to the integral (2.7). On the other hand, as discussed below, this is not the case for the plateau observed in the latter case.

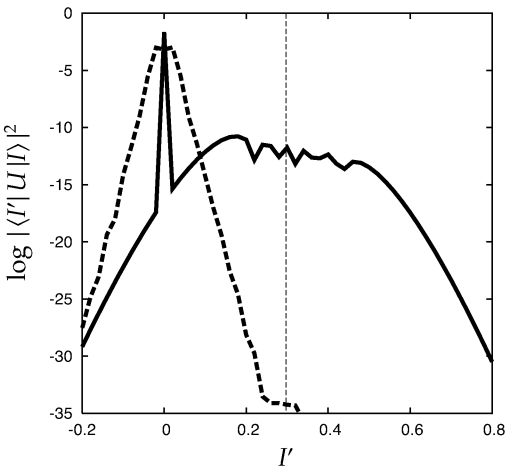

Figure 2. One-step propagator $|\langle I'|\hat{\mathcal{U}}\,|I\rangle|^2$ in the log scale. Here the initial $I = 0$ is fixed throughout and the propagator is plotted as a function of the final I'. The solid line is the case with $\beta = 1$ and the dotted one with $\beta = 50$, respectively.

§ 3. Edge contribution and diffraction

We first claim that this plateau pattern appears as a result of *diffraction*. To simplify the problem, we set our smoothness parameter as $\beta = \infty$, which brings a strict discontinuity in the kinetic term $T(p)$. To focus only on the term responsible for invoking the plateau pattern due to discontinuity, we consider the integral associated with $T_1(p)$:

$$\langle I'|\,e^{-\frac{\mathrm{i}}{\hbar}T_1(p)}\,|I\rangle = \int_{-\infty}^{\infty} dq \int_{-\infty}^{\infty} dq' \int_{-\infty}^{\infty} dp \exp\Big[-\frac{\mathrm{i}}{\hbar}\Big\{S(I',q) - S(I,q) - p(q'-q) + T_1(p)\Big\}\Big]. \tag{3.1}$$

Here we examine the case with $s = 0$ and $g \neq 0$:

$$T_1(p) = \begin{cases} 0 & (p < d) \\ g(p-d) & (p > d). \end{cases} \tag{3.2}$$

To perform the integration for p, we need to take into account a discontinuous point $p = d$, that is, the edge contribution. It is well known that for given functions

$p(z)$ and $q(z)$, under the presence of the indifferentiable point $z = d$, the lowest order contribution with respect to a large parameter η in general is evaluated as [10],

$$\left(\int_{-\infty}^{d-0} + \int_{d+0}^{\infty}\right) \mathrm{e}^{\mathrm{i}\eta p(z)} q(z) dz \simeq \frac{\mathrm{e}^{\mathrm{i}\eta p(d-0)} q(d-0)}{\mathrm{i}\eta p'(d-0)} - \frac{\mathrm{e}^{\mathrm{i}\eta p(d+0)} q(d+0)}{\mathrm{i}\eta p'(d+0)}. \tag{3.3}$$

Employing this formula, we obtain

$$\langle I' | \, e^{-\frac{\mathrm{i}}{\hbar} T_1(p)} \, | I \rangle \simeq \int_{-\infty}^{\infty} dq \int_{-\infty}^{\infty} dq' \exp\Big[\frac{\mathrm{i}}{\hbar} F(q, q')\Big] \Big(G(q, q', 0) - G(q, q', g) \Big)$$

where

$$\begin{aligned} F(q, q') &= d(q' - q) - S(I', q') + S(I, q) \\ G(q, q', \omega) &= \frac{\hbar}{\mathrm{i}(q' - q - \omega)}. \end{aligned}$$

We note that the algebraic dependence on $\hbar$ appears in $G(q, q', \omega)$, which is a typical signature of diffraction. We next perform the saddle point evaluation for integrals over q and q', which leads to

$$\begin{aligned} &\simeq (2\pi\hbar) \left| \frac{\partial^2 F(q_0, q_0')}{\partial q^2} \frac{\partial^2 F(q_0, q_0')}{\partial q'^2} \right|^{-1/2} \exp\Big[\frac{\mathrm{i}}{\hbar} F(q_0, q_0')\Big] \left(G(q_0, q_0', 0) - G(q_0, q_0', g) \right) \\ &= (2\pi \mathrm{i}\hbar^2) \big| a^2 \sin q_0 \sin q_0' \big|^{-1/2} \exp\left[\frac{\mathrm{i}}{\hbar} \Big\{ d(q_0' - q_0) - S(I', q_0') + S(I, q_0) \Big\} \right] \\ &\qquad \times \left(\frac{1}{q_0' - q_0 - g} - \frac{1}{q_0' - q_0} \right). \end{aligned} \tag{3.4}$$

For given I and I', the saddle point condition is given as

$$\cos q_0 = \frac{d - I}{a} \tag{3.5}$$

$$\cos q_0' = \frac{d - I'}{a}. \tag{3.6}$$

This is solved as

$$q_0 = \xi_0 + \mathrm{i}\eta_0 = \mathrm{i} \log \left(\frac{d}{a} + \sqrt{\Big(\frac{d}{a}\Big)^2 - 1} \right)$$

and

$$q_0' = \xi_0' + \mathrm{i}\eta_0' = \begin{cases} \mathrm{i} \log \left(\dfrac{d - I'}{a} + \sqrt{\Big(\dfrac{d - I'}{a}\Big)^2 - 1} \right) & (I' < d - a) \\ \arccos \left(\dfrac{d - I'}{a} \right) & (d - a < I' < d + a) \\ \pi + \mathrm{i} \log \left(\dfrac{I' - d}{a} + \sqrt{\Big(\dfrac{I' - d}{a}\Big)^2 - 1} \right) & (d + a < I'). \end{cases}$$

Here $I = 0$ is assumed in the final expression.

As shown in Fig. 3, the function thus obtained exhibits the plateau we have seen in Fig. 2 for $\beta = \infty$ case. Therefore, we may interpret that the plateau for large β situaitons originates from diffraction. Here the term "diffraction" is used as a phenomenon appearing when certain discontinuities cause singular scatterings in wave propagation.

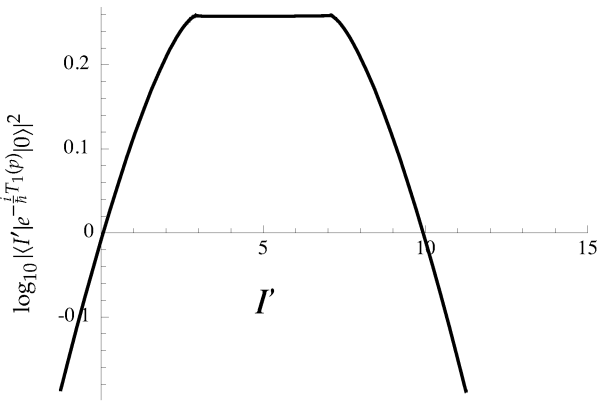

Figure 3. The semiclassical evaluation of $\langle I'|\, e^{-\frac{\mathrm{i}}{\hbar}T_1(p)}\,|I\rangle$.

§ 4. Saddle point evaluation

Next we examine the saddle point evaluation for large but finite values of β. Instead of the kinetic terms given (3.2), we use a simpler one as

$$T_1'(p) = g\theta_\beta(p-d)$$

where we first define the derivative of the kinetic term and integrate it to have

$$T_1(p) = \frac{g}{2\beta}\Big[\ \beta p + \log(\cosh(\beta p))\ \Big].$$

with $g = 1$.

The saddle point condition for one-step propagator (2.7) is then written as

$$-\frac{\partial S(I,q)}{\partial q} + p = 0, \tag{4.1}$$

$$\frac{\partial S(I',q')}{\partial q'} - p = 0, \tag{4.2}$$

$$-(q'-q) + T_1'(p) = 0, \tag{4.3}$$

which leads to the condition

$$\frac{I'-I}{a} = \cos\Big(q-\frac{\omega}{2}\Big) - \cos\Big(q-\frac{\omega}{2}+T_1'\big(I+a\cos(q-\frac{\omega}{2})\big)\Big)\,. \tag{4.4}$$

Since I and I' are observables, both should take real-valued. Thus to obtain saddle points we have to solve a shooting problem for given $I, I' \in \mathbb{R}$. Note that the resulting saddle points are not necessarily real but can be complex.

In Fig. 4, we display a set of saddle points q satisfying the condition (4.5). Here the initial state is set as $I = 0$, and the final value I' varies along each curve. In other words, the number of saddle points for a given I' corresponds to the number of curves drawn in Fig. 4. In the center of each characteristic flower-like structure, the divergent points of $I'(q)$ are located. With increase in β, divergent points of $I'(q)$ become denser, finally forming a necklace-like structure as $\beta \to \infty$.

The points satisfying the condition

$$\frac{\partial I'}{\partial q} = 0 \tag{4.5}$$

provide turning points (or caustics) in the saddle point analysis, and will play essential roles in the subsequent argument.

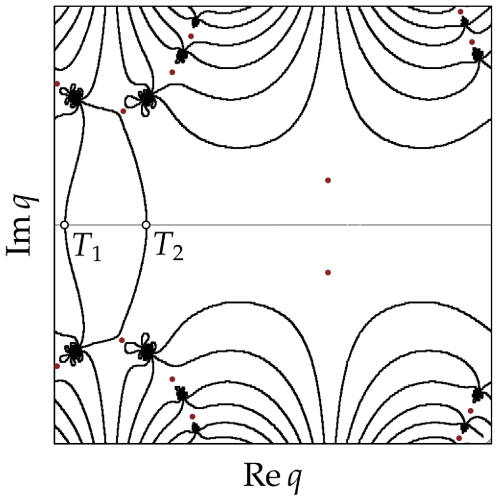

Figure 4. The set of saddle points q satisfying the condition (4.5). The open dots, denoted by T_1 and T_2, are the turning points on the real axis whereas filled ones show those in the complex plane, respectively.

It is important to remark that there are two types of turning points; the first-type, shown as open dots in Fig. 4, is located on the real axis of the complex q plane, and they are, as explained below, characterized by being locally highly degenerated, reflecting almost tangential intersection of the initial manifold I and one-step iterated manifold $F(I)$ close to the real plane. The second type is the turning points associated with divergent points of $I'(q)$, which are shown as filled dots in Fig. 4. The number of turning points of the second type grows with β as divergent points of $I'(q)$ do so. They align along the necklace structure of divergent points.

Although not shown explicitly here, the leading-order saddle point evaluation does not work and cannot reproduce the plateau with a sharp spike appearing in the large β case. In some sense it would be reasonable that the leading order semiclassical treatment does not have any capability of singular patterns shown as in Fig. 2.

§ 5. Local behaviors around two types of turning points

In what follows, we explain why the leading order treatment in the saddle point analysis does not work based on natures of two types of turning points mentioned above. First, we show the local behavior around the turning points of the first type. Figure 5 depicts the behavior of $I'(q)$ around each turning point located on the real axis. Here the final action value $I'(q)$ is plotted as a function of $\mathrm{Im}\, q$. We can clearly see that the curve becomes flatter and flatter as β increases, implying that the relation between the initial manifold I and the one-step iterated one $F(I)$ becomes close to each other.

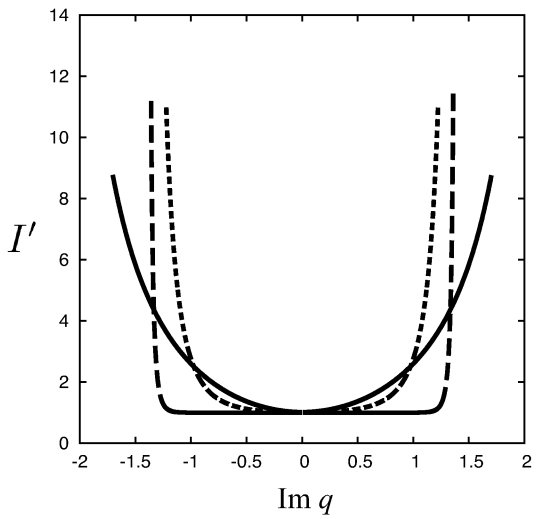

Figure 5. The behavior of $I'(q)$ around the turning point located on the real axis.

This is indeed the case, as demonstrated in Fig. 6, in which we draw the initial and final (one-step iterated) manifold in the real phase space. With increase in β, we can notice that the initial and final manifolds intersect in an almost tangential manner. In the case of $\beta = 10$, the initial manifold almost coincides with an underlying invariant manifold (Kolmogorov-Arnold-Moser curve) in phase space, meaning that it stays almost the same even after one-step iteration. As a result the initial and final manifolds intersect with each other, but only its intersection angle is very small. This causes a very flat part in the function $I'(q)$ shown in Fig. 5. Note, nevertheless, that

there always exist intersecting points between the manifolds I and $F(I)$, thereby saddle points continuously appear in the complex q plane as shown in Fig. 4.

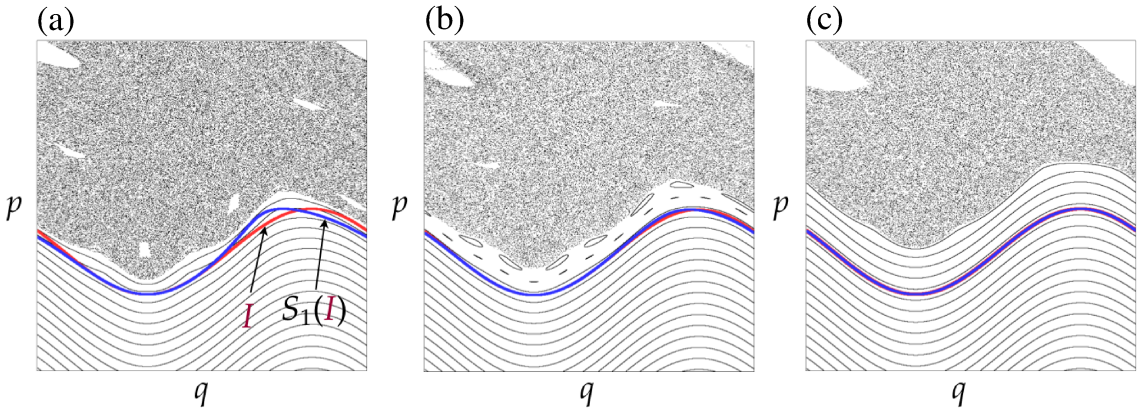

Figure 6. The initial and one-step iterated manifolds in the real phase space. The smoothness parameter is chosen as (a) $\beta = 0.1$, (b) $\beta = 1.0$ and (c) $\beta = 10$.

The local nature around the turning points are often discussed based on a series of canonical integrals as

$$\Psi_K(\mathbf{x}) = \int_{-\infty}^{\infty} \exp(\mathrm{i}\,\Phi_K(t;\mathbf{x}))\,dt \tag{5.1}$$

where the phase function is given as polynomials

$$\Phi_K(t;\mathbf{x}) = t^{K+2} + \sum_{m=1}^{K} x_m t^m\,. \tag{5.2}$$

The case $K = 1$ corresponds to the Airy integral, $K = 2$ the Pearcey integral, and so on. When all the saddles and turning points coalesce, that is $\mathbf{x} = (x_1, 0, \cdots, 0)$, the phase function $\Phi_K(t;\mathbf{x})$ around the turning point becomes flatter, like the function $I'(q)$ shown in Fig. 5. However, it should be noted that flatness of the function $I'(q)$ is more pronounced because the kinetic term $T(p)$ and the resulting saddle point condition (4.5) contains transcendental functions. In any case, as shown in Fig. 7(b), the range, in which the leading-order saddle point approximation is invalid, grows with increase in the degree K.

However, one notices that the presence of flatter regions is not enough to generate the plateau structure since, as seen in Fig. 7(b), the function is still decaying even if the degree K is increased. In other words one could not attribute the emergence of plateau only to tangential intersections of manifolds close to the real phase space. As explained below, the turning points associated with divergent points of $I'(q)$ also play a role.

Before discussing this point, we show how the manifold behaves not in close neighborhood of the real plane. In contrast to the behavior close to the real plane, the

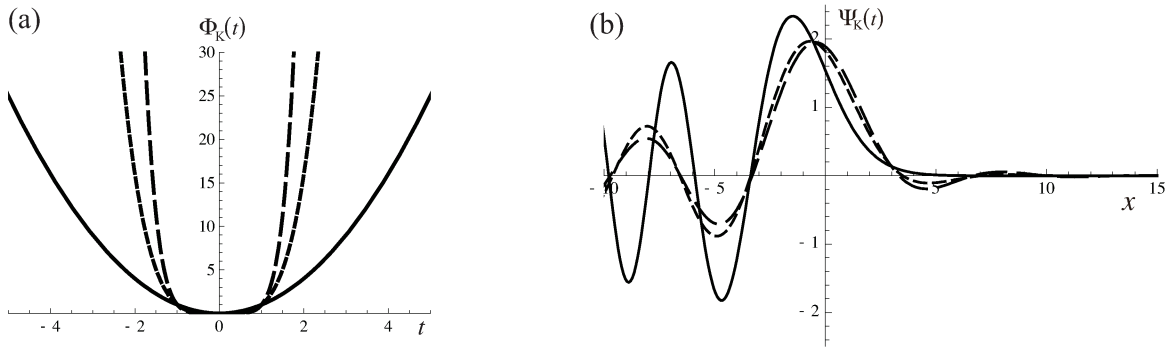

Figure 7. (a) The phase function $\Phi_K(t;\mathbf{x})$ with $\mathbf{x} = (x_1, 0, \cdots, 0)$ and (b) $\Psi_K(\mathbf{x})$ as a function of x. The solid, dotted and broken lines represent the cases with $K = 1$, $K = 5$ and $K = 9$, respectively.

manifold is violently deformed in the complex space even after one-step iteration. As shown in Fig. 8, the manifold keeps its shape in the region close to the real phase space, whereas it suffers quite large deformation in the deep complex plane.

In the $\beta = \infty$ case, there exists a strict discontinuity line at $p = d$, and so it provides a discontinuity plane as well in the complex plane. Thus a large deformation observed for large β can be regarded as a remnant of discontinuity for $\beta = \infty$. In other words, using a series of divergent points of $I'(q)$, the manifold mimics discontinuous behavior in the $\beta = \infty$ limit. As mentioned above, as the value of β grows, the divergent points become denser. Therefore, as the discrepancy between the manifold specified by I and the true invariant manifold close to the real plane gets smaller, the degree of distortion around the discontinuous plane becomes more drastic. The two tendencies are complementary to each other.

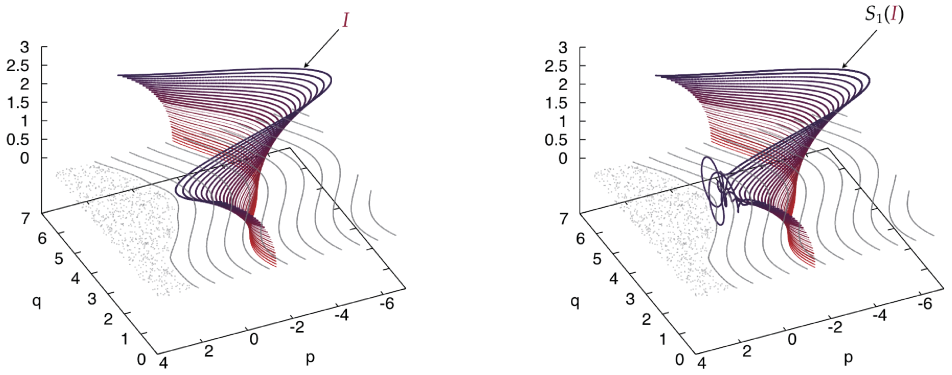

Figure 8. The initial and one-step iterated manifolds in the complex plane. The smoothness parameter is chosen as $\beta = 10$.

On the basis of our observation on the series of turning points related to large de-

formation in the complex plane, we need to argue the local signature of manifold around such turning points. With increase in β, not only the density of turning points but also the nature of manifold around individual turning point transmutes. As illustrated in Fig. 9, the manifold around individual turning point bends more sharply with β since, as mentioned above, the manifold is sharply deformed in the large β limit. As the degree of bending becomes sharper, the asymptotic region in which the leading order saddle point approximation is invalid becomes far away from the turning point, as shown in the right panel in Fig. 9, thereby the validity range of the leading order approximation shrinks.

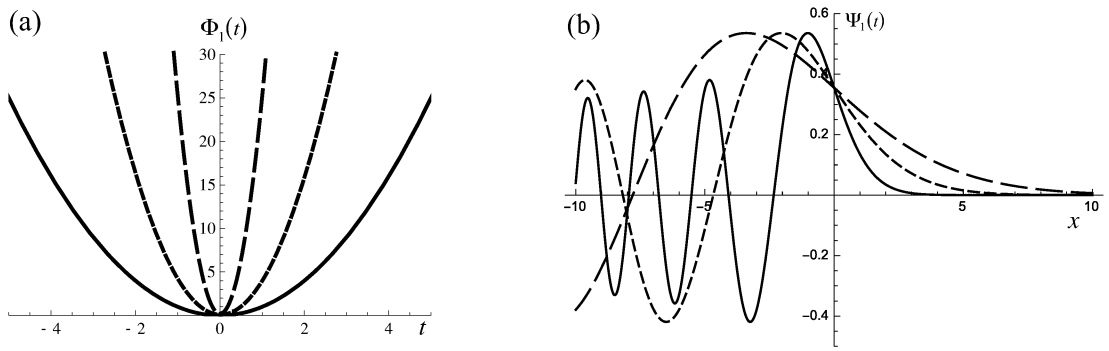

Figure 9. (a) The phase function $\Phi_1(t; a\mathbf{x})$ with $\mathbf{x} = (x_1, 0, \cdots, 0)$ and (b) $\Psi_1(a\mathbf{x})$ as a function of x. The solid, dotted and broken lines represent the cases with $a = 0.3$, $a = 0.5$ and $a = 1$, respectively.

We speculate that the plateau structure emerges as a result of combined effects of these two types of turning points. Around both types of turning points, the ranges beyond the leading order approximation get larger as β increases, and the anomalous nature of $\langle I'|\hat{\mathcal{U}}|I\rangle$ appears exactly in the region sandwiched between two types of turning points.

§ 6. Outlooks

Diffraction invoked in the present model would not be surprising in some sense since discontinuity was introduced by hand in the model. The breakdown of the leading order saddle point approximation for large β cases is therefore expected on the same footing. However, as will be reported elsewhere [11], we encounter quite similar situations in analytic maps such as the standard map if we take appropriately tuned representations as initial and final states. In the treatment performed in [11], instead of varying the smoothness parameter β, we adjust the initial and final manifolds which provide good approximations to the underlying invariant curves. This is achieved by preparing completely integrable Hamiltonians. Under such representations, one-step

propagator exhibits similar anomalous behavior as illustrated in Fig. 2, and the saddle point approximation does not work there in the leading order as is the present case. Two types of turning points also appear and the underlying mechanism looks common to the present situation. If our argument developed here holds for the analytic map as well, it turns out that the purely quantum transition from one invariant curve in phase space to another should be regarded as diffraction, not tunneling, even in generic situations. This may enforce to change our perspective to dynamical tunneling considerably.

References

[1] Creagh S C 1998 Tunneling in two dimensions in *Tunneling in Complex Systems*, edited by S. Tomsovic, (World Scientific, Singapore) pp 35–100
[2] Keshavamurthy S and Schlagheck P 2011 *Dynamical Tunneling: Theory and Experiment* (CRC Press)
[3] Shudo A and Ikeda K S 1995 Complex classical trajectories and chaotic tunneling Phys. Rev. Lett. **74** 682–85
[4] Shudo A and Ikeda K S 1998 Chaotic tunneling: A remarkable manifestation of complex dynamical system in nonintegrable quantum phenomena Physica D **115** 234–292
[5] Shudo A, Ishii Y and Ikeda K S 2002 Julia set describes quantum tunneling in the presence of chaos J. Phys. A. **35** L225–31
[6] Shudo A, Ishii Y and Ikeda K S 2008 Julia sets and chaotic tunneling I J. Phys. A: Math. Theor. **42** 265101 (26 pages)
[7] Shudo A, Ishii Y and Ikeda K S 2008 Julia sets and chaotic tunneling II J. Phys. A: Math. Theor. **42** 265102 (34 pages)
[8] Hanada Y, Shudo A and Ikeda K S 2015 Origin of the enhancement of tunneling probability in the nearly integrable system Phys. Rev. E, **91** 042913 (16 pages)
[9] Ishikawa A, Tanaka A, Ikeda K S and Shudo A 2012 Diffraction and tunneling in systems with mixed phase space Phys. Rev. E. **86** 036208 (14 pages)
[10] Olver F W J 1974 *Asymptotics and special functions*, (New York, NY : Academic Press)
[11] Shudo A, Hanada Y and Ikeda K S in preparation